

# Polymer stabilized chiral nematic liquid crystals for fast switching and high contrast electro-optic devices

Damian J. Gardiner,<sup>1,a)</sup> Stephen M. Morris,<sup>1</sup> Flynn Castles,<sup>1</sup> Malik M. Qasim,<sup>1</sup> Wook-Sung Kim,<sup>2</sup> Su Seok Choi,<sup>2,a)</sup> Hyun-Jin Park,<sup>2</sup> In-Jae Chung,<sup>2</sup> and Harry J. Coles<sup>1,a)</sup>

<sup>1</sup>Centre of Molecular Materials for Photonics and Electronics, Electrical Engineering Division, University of Cambridge, 9 JJ Thomson Avenue, Cambridge CB3 0FA, United Kingdom

<sup>2</sup>LG Display, R&D Center, 1007, Deogeun-ri, Wollong-myeon, Paju-si, Gyeonggi-do 413-811, Korea

(Received 28 March 2011; accepted 2 June 2011; published online 30 June 2011)

A fast switching electro-optic device, based upon the in-plane addressing of very short pitch polymer stabilized chiral nematic liquid crystals, is presented. Polymer stabilization of the standing helical arrangement is essential to prevent the appearance of defects above the in-plane electrodes. Response times as short as 50  $\mu\text{s}$  are observed at room temperature along with contrast ratios greater than 3000:1 owing to the high optical extinction at visible wavelengths in the “Off” state. The combination of these fast response times with such high contrast ratios is of great importance for next generation electro-optical elements. © 2011 American Institute of Physics. [doi:10.1063/1.3605597]

For many future display applications of liquid crystals (LCs), the main disadvantage of existing nematic technology remains the relatively slow response due to the viscoelastic relaxation of the LC. This response is a limiting factor for applications into next generation display devices. To improve the response time, some recent work on faster switching LC modes has included polymer stabilized “blue-phase” mode and chiral nanostructured devices.<sup>1–3</sup> These devices require some special processing conditions in order to function effectively, such as ultraviolet curing at a precise temperature within the LC blue phase or isotropic phase.

Recently, chiral nematic LCs have been examined whereby the helicoidal pitch is made sufficiently small so as to reduce the transmission of light when the sample is sandwiched between crossed polarizers, and the helical axis is perpendicular to the substrate in the uniform standing helix (USH) geometry.<sup>4–9</sup> This can lead to significant improvements in the contrast ratio due to the very low transmission of light in the “Off” state,  $T_{\text{off}}$ . The pitch,  $P$ , must be made as small as possible since, theoretically, in this geometry,  $T_{\text{off}}$  can be expressed as<sup>7</sup>

$$T_{\text{off}} \approx \frac{\pi^2 \bar{n}^4 (\Delta n)^4 P^6 d^2}{16\lambda^8}, \quad (1)$$

where  $\bar{n}$  is the average of the principal refractive indices ( $(n_{\parallel} + n_{\perp})/2$ ) whereby  $n_{\parallel}$  and  $n_{\perp}$  are the refractive indices parallel and perpendicular to the local director),  $d$  is the cell gap,  $\Delta n$  is the birefringence ( $n_{\parallel} - n_{\perp}$ ), and  $\lambda$  is the incident wavelength. Potential devices have been proposed using the flexoelectro-optic effect<sup>7</sup> or dielectrically driven out-of-plane rotation of the helical axis using negative dielectric anisotropy materials.<sup>9</sup>

In this letter, we present results on a device that exhibits electro-optic switching with response times less than 100  $\mu\text{s}$  for full intensity modulation. The device is based upon

in-plane addressing of very short pitch polymer stabilized chiral nematic LCs using a commercial in-plane switching (IPS) cell architecture. Application of an electric field induces a birefringent, transmissive, on-state. Coupled with the very low transmission in the off-state, due to the short pitch chiral LC, this allows the possibility of generating extremely high contrast devices with very fast response.

A schematic of the IPS test cell consisting of indium tin oxide inter-digitated electrodes is shown in Fig. 1. The electrode width is  $w = 4 \mu\text{m}$ , electrode separation is  $s = 9 \mu\text{m}$ , and cell gap is  $d = 5 \mu\text{m}$ . Chiral nematic mixtures consisting of the commercial mixture, MDA-00-3506 (Merck KGaA) and  $\approx 7$  wt. % of the high-twisting power ( $>80 \mu\text{m}^{-1}$ ) chiral dopant (R-5011, Merck KGaA), were prepared. The concentration of chiral dopant was chosen such that it positioned the reflection band at wavelengths shorter than the visible regime ( $P < 220 \text{ nm}$ ). The birefringence and dielectric anisotropy of the host compound were  $\Delta n = 0.25$  (measured at  $\lambda = 589.8 \text{ nm}$ ) and  $\Delta\epsilon = 41.6$ , respectively, at a temperature of 20 °C.

When an electric field was applied to a chiral nematic IPS cell, it was found that significant hysteresis was observed in the switching due to defect formation above the IPS electrodes. To alleviate this problem, we have discovered that it is essential to polymer stabilize the IPS device using 7 wt. % of the reactive mesogen RM-257 (Merck, KGaA) and 0.7 wt. % photoinitiator (IC-819, Ciba-Geigy). Polymer stabilization is a technique previously used to enhance or retain LC alignment.<sup>10</sup> Samples were capillary filled and ultraviolet cured (Exfo Omnicure S1000,  $\lambda = 365 \text{ nm}$ , exposure 5  $\text{mW}/\text{cm}^2$  for 15 min at room temperature). Further details of the defect formation and polymer stabilization procedure are to be discussed elsewhere.<sup>11</sup> The microscope-based electro-optic rig and experimental acquisition apparatus are described in Ref. 6.

Figure 2(a) shows the T-E curve as a function of electric field for three different wavelengths, corresponding to red ( $\lambda = 658 \text{ nm}$ ), green ( $\lambda = 546 \text{ nm}$ ), and blue ( $\lambda = 436 \text{ nm}$ ) light. The appropriate wavelength range was selected by use of narrow band pass filters with  $\Delta\lambda = 10 \text{ nm}$ . In all cases, the square-wave (1 kHz) electric field was increased at a constant ramp rate of 0.5  $\text{V}/\mu\text{m}$  per second. At low field

<sup>a)</sup>Authors to whom correspondence should be addressed. Electronic addresses: djg47@eng.cam.ac.uk, aiconess@lgdisplay.com, and hjc37@cam.ac.uk.

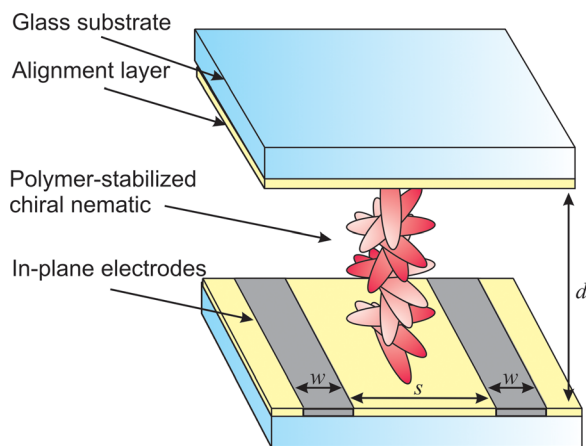


FIG. 1. (Color online) Schematic of the electro-optic cell architecture.

strengths, the transmission is low, subsequently rising nonlinearly with increasing field strength. For the three T-E curves, the “On” state applied electric field strength,  $E_{\text{on}}$ , (full-intensity modulation) was found to be  $24.8 \text{ V}/\mu\text{m}$ ,  $20.8 \text{ V}/\mu\text{m}$ , and  $17.4 \text{ V}/\mu\text{m}$  for red, green, and blue light, respectively. The inset of Fig. 2(a) shows that, on increasing and decreasing the electric field strength, there is minimal

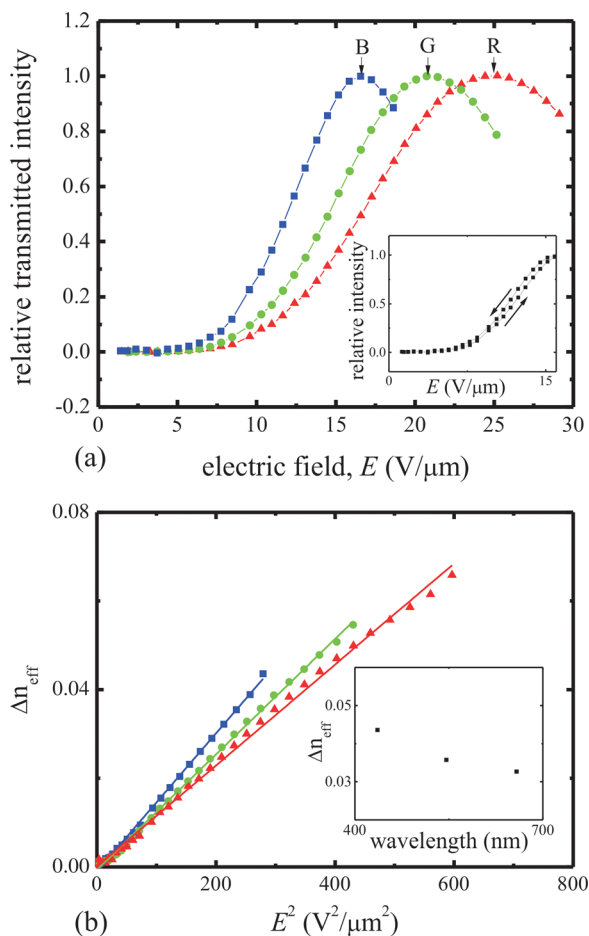


FIG. 2. (Color online) (a) Relative transmitted intensity as a function of electric field measured at 436 nm (squares), 546 nm (circles), and 658 nm (triangles), respectively. The inset shows the reproducible switching on field ramp reversal. (b) Plots of  $\Delta n_{\text{eff}}$  against  $E^2$  for each wavelength; the inset shows  $\Delta n_{\text{eff}}$  as a function of wavelength for a fixed applied electric field of  $16.4 \text{ V}/\mu\text{m}$ .

hysteresis (i.e.,  $< \pm 5\%$ ), furthermore the original “Off” state is fully recovered.

The data may be approximately described by the relative transmitted intensity  $T$  through a uniaxially birefringent slab

$$T = \sin^2(2\Psi)\sin^2\left(\frac{\pi\Delta n_{\text{eff}}d}{\lambda}\right). \quad (2)$$

Here,  $\Delta n_{\text{eff}}$  is the *effective* induced birefringence at a particular applied electric field strength and  $\Psi$  is the angle of the induced, in-plane, optic axis with respect to the polarizer/analyzer crossed axis ( $\Psi = 45^\circ$  in this work). From this, it is found that  $\Delta n_{\text{eff}}$  is approximately proportional to the square of the applied electric field (Fig. 2(b)). A small structured residual is also apparent, indicating the presence of non-quadratic terms. A plot of  $\Delta n_{\text{eff}}$  as a function of wavelength, which shows typical Cauchy-like dispersion behaviour, is shown in the inset to Fig. 2(b).

The quadratic dependency of the birefringence on the electric field is typical for dielectric coupling; however, in this USH geometry, the flexoelectric coupling is also expected to give a similar dependency at low field strengths (Eq. (17) in Ref. 7). Previous work has shown that both dielectric and flexoelectric coupling can contribute to an induced optic axis.<sup>12</sup> Further work is underway to determine the relative contribution of both mechanisms.

By observing an isolated train of 3 bipolar pulses, the rise and decay times (each measured considering a 10%–90% change of the transmitted intensity, respectively) as a function of the electric field strength were obtained at a constant temperature of  $30^\circ\text{C}$  using  $\lambda = 436 \text{ nm}$ . These are plotted in Fig. 3 with a typical optical response shown in the inset. It is believed that the small dips shown in the optical response, when the drive signal changes polarity, are caused by a combination of both flexoelectric and dielectric switching at the zero-field crossover point. From Fig. 3, the rise time reduces significantly with increasing electric field strength, decreasing from  $125 \mu\text{s}$  at  $13 \text{ V}/\mu\text{m}$  to  $50 \mu\text{s}$  at  $17.4 \text{ V}/\mu\text{m}$ . The decay time increases slowly from  $30 \mu\text{s}$  to  $60 \mu\text{s}$  from  $13 \text{ V}/\mu\text{m}$  and  $17.4 \text{ V}/\mu\text{m}$ , respectively. These fast

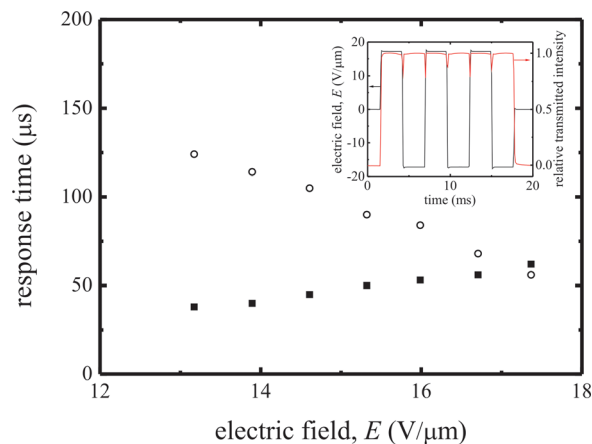


FIG. 3. (Color online) Response times of the USH cell as a function of electric field strength (rise time (open circles) and decay time (closed squares)) measured at  $30^\circ\text{C}$  and  $436 \text{ nm}$  wavelength. The inset shows the optical response (plotted on the secondary axis) for an isolated train of 3 bipolar pulses.

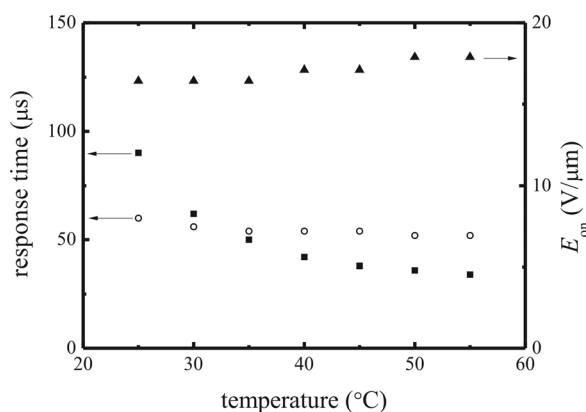


FIG. 4. The temperature dependence of the electro-optic characteristics ( $\lambda = 436$  nm). The rise (open circles) and decay (closed squares) times as a function of temperature for  $E = 17.4$  V  $\mu\text{m}^{-1}$  are plotted on the primary axis. The value of  $E_{on}$  for the first bright state is plotted on the secondary axis (closed triangles).

response times are of considerable importance with regards to minimizing motion blur and enabling frame sequential color in a practical display.

The temperature dependence of the T-E properties and response times were examined over a range from 25 °C to 55 °C, Fig. 4.  $E_{on}$  appears to be approximately temperature independent over this range, varying by less than 10%. The rise and decay times as a function of temperature for  $E = 17.4$  V/ $\mu\text{m}$  are also shown. Both response times decrease as the temperature is increased although the effect is more pronounced for the decay time. For example, the rise time decreases steadily from around 60  $\mu\text{s}$  at 25 °C to only 50  $\mu\text{s}$  at 55 °C. The decay times, on the other hand, decrease more rapidly from 90  $\mu\text{s}$  to 34  $\mu\text{s}$  with an Arrhenius-like dependence on temperature as the viscosity decreases with increasing temperature.

Photographs of the “Off” (zero field) and “On” states are shown in Fig. 5. The images were taken after 100 repeated scans of the electric field and there was no change in the appearance of the sample. Consequently, the USH device retains the high extinction “Off” state of the highly twisted chiral nematic LC. The contrast ratio, measured with a calibrated photometer at normal incidence, was in excess of 3000:1 and the off state transmission was 0.7 nt.

In summary, a fast-switching, high contrast electro-optic element based upon in-plane addressing of a polymer-stabilized hyper twisted chiral nematic LC has been presented. The device switches from a dark state to a transmissive state through an electrically induced birefringence. Polymer stabilization of the texture is essential for the device to function by inhibiting defect formation above the electrodes. Response times as low as 50  $\mu\text{s}$  at room temperature were reported and thus this device offers significant potential for applications where a very fast response is required, such as

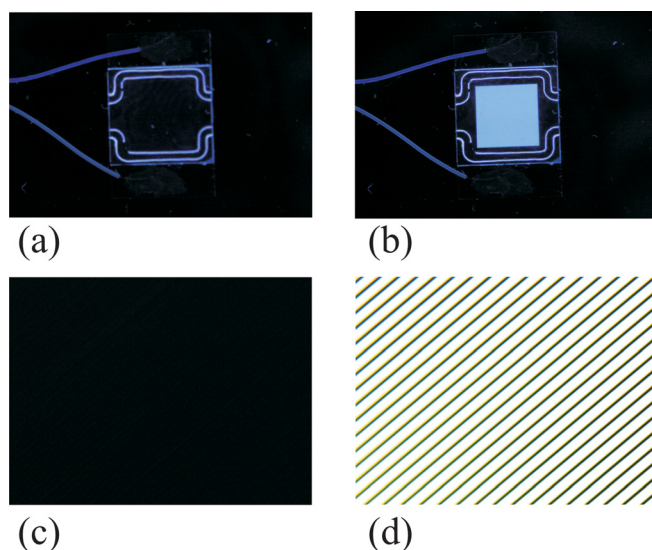


FIG. 5. (Color online) Photographs of (a) “Off” and (b) “On” state of the USH cell on a cold-cathode fluorescence backlight between crossed polarizers. The electrode region covers an active area of 1 cm<sup>2</sup>. The “Off” (c) and “On” (d) states recorded using a polarizing microscope. The dark lines in (d) represent the regions above the electrodes, which are  $w = 4$   $\mu\text{m}$ . The in-plane electrode separation is  $s = 9$   $\mu\text{m}$ .

next generation frame sequential colour displays and phase change telecommunication devices. Further work is in progress to reduce driving voltages through materials and polymerization process optimization.

W.S.K., S.S.C., H.J.P., and I.J.C. would like to thank Dong-Guk Kim, Jonghoon Woo, Dong-Jin Kim, Myung-Su Yang, and Yong-Kee Whang of LGD for supporting this work.

<sup>1</sup>H. Kikuchi, M. Yokota, Y. Hisakado, H. Yang, and T. Kajiyama, *Nat. Mater.* **1**, 64 (2002).

<sup>2</sup>Y. Haseba, H. Kikuchi, T. Nagamura, and T. Kajiyama, *Adv. Mater.* **17**, 2311 (2005).

<sup>3</sup>J. Yan, H.-C. Cheng, S. Gauza, Y. Li, M. Jiao, L. Rao, and S.-T. Wu, *Appl. Phys. Lett.* **96**, 071105 (2010).

<sup>4</sup>H. H. Lee, J.-S. Yu, J.-H. Kim, S.-I. Yamamoto, and H. Kikuchi, *J. Appl. Phys.* **106**, 014503 (2009).

<sup>5</sup>H. J. Coles, M. J. Coles, B. J. Broughton, and S. M. Morris, European patent EP1766461B (2 July 2009).

<sup>6</sup>B. J. Broughton, M. J. Clarke, A. E. Blatch, and H. J. Coles, *J. Appl. Phys.* **98**, 034109 (2005).

<sup>7</sup>F. Castles, S. M. Morris, and H. J. Coles, *Phys. Rev. E* **80**, 031709 (2009).

<sup>8</sup>F. Castles, S. M. Morris, D. J. Gardiner, Q. M. Malik, and H. J. Coles, *J. Soc. Inf. Disp.* **18**, 128 (2010).

<sup>9</sup>S. S. Choi, F. Castles, S. M. Morris, and H. J. Coles, *Appl. Phys. Lett.* **95**, 193502 (2009).

<sup>10</sup>I. Dierking, *Adv. Mater.* **12**, 167 (2000).

<sup>11</sup>D. J. Gardiner, S. M. Morris, F. Castles, and H. J. Coles, *The effect of in-plane electric fields on chiral nematic liquid crystals in the uniform standing helix configuration* (unpublished).

<sup>12</sup>A. J. Davidson, S. J. Elston, and E. P. Raynes, *J. Appl. Phys.* **99**, 093109 (2006).